

DAVID W. TAYLOR NAVAL SHIP RESEARCH AND DEVELOPMENT CENTER

Bethesda, Maryland 20084



JAN 82

INVESTIGATION OF THE HYDRODYNAMIC LOADING ON RIBBON TOWCABLE

Reece Folb
John Nelligan

WHOI
DOCUMENT
COLLECTION

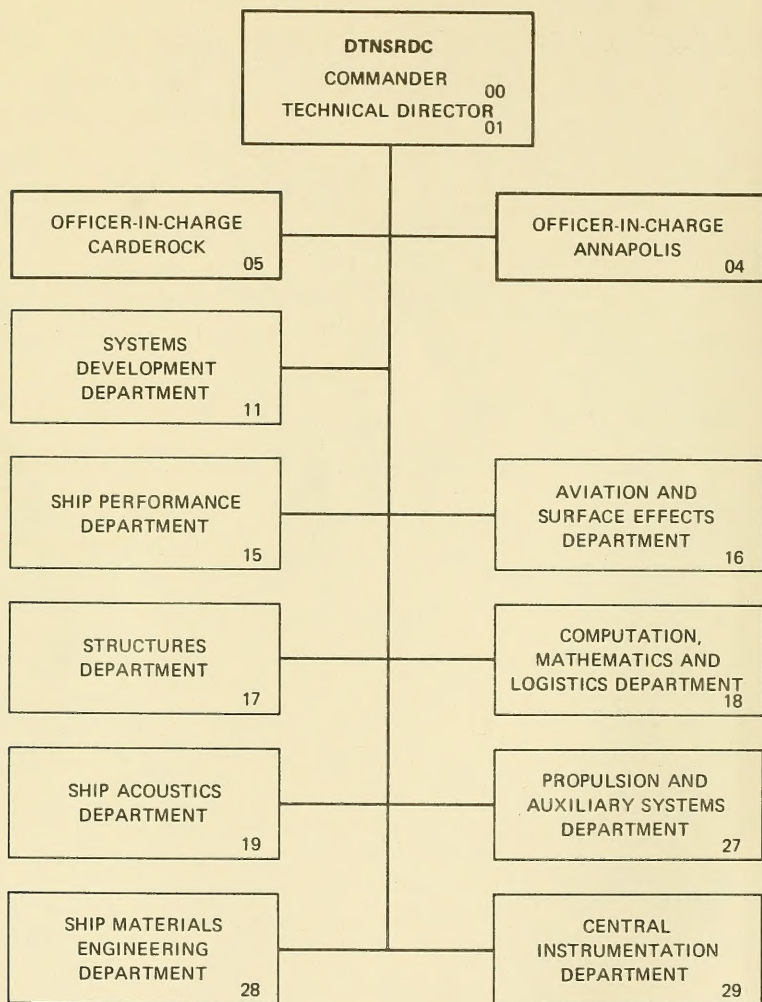
APPROVED FOR PUBLIC RELEASE; DISTRIBUTION UNLIMITED

SHIP PERFORMANCE DEPARTMENT
DEPARTMENTAL REPORT

January 1982

DTNSRDC/SPD 1030-01

MAJOR DTNSRDC ORGANIZATIONAL COMPONENTS



MBL/WHOI



UNCLASSIFIED

SECURITY CLASSIFICATION OF THIS PAGE (When Data Entered)

REPORT DOCUMENTATION PAGE		READ INSTRUCTIONS BEFORE COMPLETING FORM
1. REPORT NUMBER DTNSRDC/SPD 1030-01	2. GOVT ACCESSION NO.	3. RECIPIENT'S CATALOG NUMBER
4. TITLE (and Subtitle) INVESTIGATION OF THE HYDRODYNAMIC LOADING ON RIBBON TOWCABLE		5. TYPE OF REPORT & PERIOD COVERED DEPARTMENTAL
		6. PERFORMING ORG. REPORT NUMBER DTNSRDC/SPD 1030-01
7. AUTHOR(s) Reece Folb and John Nelligan		8. CONTRACT OR GRANT NUMBER(s)
9. PERFORMING ORGANIZATION NAME AND ADDRESS David Taylor Naval Ship R&D Center Ship Performance Department Bethesda, MD 20084		10. PROGRAM ELEMENT, PROJECT, TASK AREA & WORK UNIT NUMBERS Element 62543N SF 43-400-001 DTNSRDC WU 1507-101
11. CONTROLLING OFFICE NAME AND ADDRESS Naval Sea Systems Command Washington, DC 20362		12. REPORT DATE January 1982
		13. NUMBER OF PAGES 27
14. MONITORING AGENCY NAME & ADDRESS (if different from Controlling Office)		15. SECURITY CLASS. (of this report) UNCLASSIFIED
		15a. DECLASSIFICATION/DOWNGRADING SCHEDULE
16. DISTRIBUTION STATEMENT (of this Report) APPROVED FOR PUBLIC RELEASE; DISTRIBUTION UNLIMITED		
17. DISTRIBUTION STATEMENT (of the abstract entered in Block 20, if different from Report)		
18. SUPPLEMENTARY NOTES		
19. KEY WORDS (Continue on reverse side if necessary and identify by block number) Ribbioned Towcables Ribbon Fairing Loading Functions Towcable Performance Improvement		
20. ABSTRACT (Continue on reverse side if necessary and identify by block number) Hydrodynamic loading functions and drag coefficients have been developed for a ribbon towcable. These functions represent a mathematical fit to data measured on a towcable at sea. The functions should be used with caution in predicting the towing configuration of other types of ribbon cable design or other cable diameters because of the difficulty in scaling ribbon characteristics such as material stiffness.		

REPORT DOCUMENTATION PAGE	
1. AGENCY USE ONLY (Leave blank)	
2. AUTHOR (Last, first, middle initial)	
3. TITLE (and Subtitle)	
4. NUMBERED LIST OF ILLUSTRATIONS	
5. AUTHOR'S ADDRESS (Organization, address, city, state, and ZIP code)	
6. AUTHOR'S REPORT NUMBER	
7. AUTHOR'S REPORT DATE	
8. AUTHOR'S REPORT TYPE AND DATES COVERED	
9. PERFORMING ORGANIZATION NAME(S) AND ADDRESS(ES)	
10. PERFORMING ORGANIZATION REPORT NUMBER	
11. PERFORMING ORGANIZATION DATE	
12. PERFORMING ORGANIZATION TYPE AND DATES COVERED	
13. PERFORMING ORGANIZATION REPORT NUMBER	
14. PERFORMING ORGANIZATION DATE	
15. PERFORMING ORGANIZATION TYPE AND DATES COVERED	
16. PERFORMING ORGANIZATION REPORT NUMBER	
17. PERFORMING ORGANIZATION DATE	
18. PERFORMING ORGANIZATION TYPE AND DATES COVERED	
19. PERFORMING ORGANIZATION REPORT NUMBER	
20. PERFORMING ORGANIZATION DATE	
21. PERFORMING ORGANIZATION TYPE AND DATES COVERED	
22. PERFORMING ORGANIZATION REPORT NUMBER	
23. PERFORMING ORGANIZATION DATE	
24. PERFORMING ORGANIZATION TYPE AND DATES COVERED	
25. PERFORMING ORGANIZATION REPORT NUMBER	
26. PERFORMING ORGANIZATION DATE	
27. PERFORMING ORGANIZATION TYPE AND DATES COVERED	
28. PERFORMING ORGANIZATION REPORT NUMBER	
29. PERFORMING ORGANIZATION DATE	
30. PERFORMING ORGANIZATION TYPE AND DATES COVERED	
31. PERFORMING ORGANIZATION REPORT NUMBER	
32. PERFORMING ORGANIZATION DATE	
33. PERFORMING ORGANIZATION TYPE AND DATES COVERED	
34. PERFORMING ORGANIZATION REPORT NUMBER	
35. PERFORMING ORGANIZATION DATE	
36. PERFORMING ORGANIZATION TYPE AND DATES COVERED	
37. PERFORMING ORGANIZATION REPORT NUMBER	
38. PERFORMING ORGANIZATION DATE	
39. PERFORMING ORGANIZATION TYPE AND DATES COVERED	
40. PERFORMING ORGANIZATION REPORT NUMBER	
41. PERFORMING ORGANIZATION DATE	
42. PERFORMING ORGANIZATION TYPE AND DATES COVERED	
43. PERFORMING ORGANIZATION REPORT NUMBER	
44. PERFORMING ORGANIZATION DATE	
45. PERFORMING ORGANIZATION TYPE AND DATES COVERED	
46. PERFORMING ORGANIZATION REPORT NUMBER	
47. PERFORMING ORGANIZATION DATE	
48. PERFORMING ORGANIZATION TYPE AND DATES COVERED	
49. PERFORMING ORGANIZATION REPORT NUMBER	
50. PERFORMING ORGANIZATION DATE	
51. PERFORMING ORGANIZATION TYPE AND DATES COVERED	
52. PERFORMING ORGANIZATION REPORT NUMBER	
53. PERFORMING ORGANIZATION DATE	
54. PERFORMING ORGANIZATION TYPE AND DATES COVERED	
55. PERFORMING ORGANIZATION REPORT NUMBER	
56. PERFORMING ORGANIZATION DATE	
57. PERFORMING ORGANIZATION TYPE AND DATES COVERED	
58. PERFORMING ORGANIZATION REPORT NUMBER	
59. PERFORMING ORGANIZATION DATE	
60. PERFORMING ORGANIZATION TYPE AND DATES COVERED	
61. PERFORMING ORGANIZATION REPORT NUMBER	
62. PERFORMING ORGANIZATION DATE	
63. PERFORMING ORGANIZATION TYPE AND DATES COVERED	
64. PERFORMING ORGANIZATION REPORT NUMBER	
65. PERFORMING ORGANIZATION DATE	
66. PERFORMING ORGANIZATION TYPE AND DATES COVERED	
67. PERFORMING ORGANIZATION REPORT NUMBER	
68. PERFORMING ORGANIZATION DATE	
69. PERFORMING ORGANIZATION TYPE AND DATES COVERED	
70. PERFORMING ORGANIZATION REPORT NUMBER	
71. PERFORMING ORGANIZATION DATE	
72. PERFORMING ORGANIZATION TYPE AND DATES COVERED	
73. PERFORMING ORGANIZATION REPORT NUMBER	
74. PERFORMING ORGANIZATION DATE	
75. PERFORMING ORGANIZATION TYPE AND DATES COVERED	
76. PERFORMING ORGANIZATION REPORT NUMBER	
77. PERFORMING ORGANIZATION DATE	
78. PERFORMING ORGANIZATION TYPE AND DATES COVERED	
79. PERFORMING ORGANIZATION REPORT NUMBER	
80. PERFORMING ORGANIZATION DATE	
81. PERFORMING ORGANIZATION TYPE AND DATES COVERED	
82. PERFORMING ORGANIZATION REPORT NUMBER	
83. PERFORMING ORGANIZATION DATE	
84. PERFORMING ORGANIZATION TYPE AND DATES COVERED	
85. PERFORMING ORGANIZATION REPORT NUMBER	
86. PERFORMING ORGANIZATION DATE	
87. PERFORMING ORGANIZATION TYPE AND DATES COVERED	
88. PERFORMING ORGANIZATION REPORT NUMBER	
89. PERFORMING ORGANIZATION DATE	
90. PERFORMING ORGANIZATION TYPE AND DATES COVERED	
91. PERFORMING ORGANIZATION REPORT NUMBER	
92. PERFORMING ORGANIZATION DATE	
93. PERFORMING ORGANIZATION TYPE AND DATES COVERED	
94. PERFORMING ORGANIZATION REPORT NUMBER	
95. PERFORMING ORGANIZATION DATE	
96. PERFORMING ORGANIZATION TYPE AND DATES COVERED	
97. PERFORMING ORGANIZATION REPORT NUMBER	
98. PERFORMING ORGANIZATION DATE	
99. PERFORMING ORGANIZATION TYPE AND DATES COVERED	
100. PERFORMING ORGANIZATION REPORT NUMBER	

TABLE OF CONTENTS

	<u>Page</u>
LIST OF FIGURES	iii
LIST OF TABLES.	iv
NOTATION.	v
ABSTRACT.	1
ADMINISTRATIVE INFORMATION.	1
INTRODUCTION.	1
BASIC CONSIDERATIONS.	2
DESCRIPTION OF EXPERIMENTAL EQUIPMENT	5
DESCRIPTION OF INSTRUMENTATION.	13
EXPERIMENTAL ARRANGEMENT AND PROCEDURES	14
RESULTS AND DISCUSSION.	14
CONCLUSIONS	21
REFERENCES.	21
APPENDIX A - A COMPARISON OF THE HYDRODYNAMIC LOADING FUNCTIONS WITH SOME CRITICAL ANGLE TOWING DATA.	22

LIST OF FIGURES

1 - DTNSRDC Depressor.	7
2 - Dimensions of DTNSRDC Depressor.	7
3 - Depressor Performance as a Function of Speed 3(a)-Cable Angle at the Depressor; 3(b)-Cable Tension at the Depressor	9
4 - Ribbon Towcable.	11
5 - Schematic Diagram of the Towing Arrangement.	15
6 - Cable Tension at the Ship as a Function of Cable Scope	16
7 - Depressor Depth as a Function of Cable Scope	17
8 - Hydrodynamic Loading Functions 8(a)-Normal Hydrodynamic Loading Function vs Cable Angle; 8(b)-Tangential Hydrodynamic Loading Function vs Cable Angle	18
9 - Drag Coefficient C_R as a Function of Reynolds Number	19
A.1- Towcable Tension per Unit Length versus Towspeed for Various Towcables.	23
A.2- Towing Angles versus Towspeed for Various Towcables.	23
A.3- Tangential Hydrodynamic Loading vs Cable Angle	27

LIST OF TABLES

Page

1 - Cable and Ribbon Geometry.	5
2 - Measurement Sensors.	13
A.1- Ribbon Configurations.	22
A.2- Derived Normal Drag Coefficients	24
A.3- Tangential Hydrodynamic Loading Values	25

NOTATION

A_o, A_1	Dimensionless coefficients
C_R	Normal drag coefficient based on cable diameter
d, D	Diameter
F	Normal component of hydrodynamic force per unit length
f_n	Normal hydrodynamic loading function
f_t	Tangential hydrodynamic loading function
G	Tangential component of hydrodynamic force per unit length
P	Tangential component of force per unit length
Q	Normal component of force per unit length
R	Cable drag per unit length when the axis is 90^0 to the flow
R_e	Reynolds number
s	Cable scope
T	Cable tension
V	Velocity
w	Cable weight per unit length in seawater
ρ	Density of seawater
ϕ	Towcable angle relative to horizontal
ϕ_c	Towcable critical angle

ABSTRACT

Hydrodynamic loading functions and drag coefficients have been developed for a ribbon towcable. These functions represent a mathematical fit to data measured on a towcable at sea. The functions should be used with caution in predicting the towing configurations of other types of ribbon cable design or other cable diameters because of the difficulty in scaling ribbon characteristics such as material stiffness.

ADMINISTRATIVE INFORMATION

The work described in this report was performed in support of a number of projects sponsored by the Naval Sea Systems Command, the Naval Ship Engineering Center and the Naval Air Systems Command. The effort was carried out jointly by David Taylor Naval Ship Research and Development Center under Program Element Number 62543N, Task Area Number SF 43-400-001, Work Unit Number 1507-101 and MAR Associates, Inc. under DTNSRDC Contract Number N00600-79-D-2507. J. Nelligan is with MAR Associates, Inc. of Rockville, Maryland.

INTRODUCTION

Various devices can be attached to round towcables to improve hydrodynamic performance. A streamlined fairing reduces the normal component of drag allowing the towline to span a greater depth per unit of scope, at the same time reducing cable strumming. Fairing, however, is expensive and can be difficult to store and stream reliably, especially in certain applications, e.g., submarine towed systems.

Ribbon towcable does not have the hydrodynamic efficiency of streamlined fairing, but it is much more easily stored and handled, in addition to being less costly. Ribbon is used primarily to reduce cable strumming which can be a source of noise or cause early fatigue. In so doing it appears also to reduce the normal component of drag below that of the fully strumming bare round cable. The mechanism by which strumming is suppressed is not fully understood but is thought to involve the disruption of spanwise coherence in vortex shedding and drag damping. A negative in the use of ribbon as with all cable-attached devices is the increase in the tangential component of drag (tension) relative to bare cable.

As ribbon towable has found important applications in fleet systems, particularly in submarine towed communications buoys and various airborne mine countermeasure systems, the need for accurate towing configuration prediction has increased. Knowing the hydrodynamic loading on the ribbon cable is required for configuration prediction.

Typically one of two methods is used by the David Taylor Naval Ship Research and Development Center (DTNSRDC) to develop the hydrodynamic loading functions. The first involves direct measurement of the hydrodynamic loading on a two-dimensional (rigid) model in the towing basin.¹ In the second technique an at-sea experiment is performed in which certain parameters describing the towing configuration are measured and the hydrodynamic loading functions are deduced by a regression analysis process until a match of computed and measured configurations is attained.

This latter technique was used to determine the hydrodynamic loading functions for a particular ribbon cable. This report describes the at-sea experiment including towable model, instrumentation, and experimental procedures; presents the results of the sea-trial and loading function analysis; and presents conclusions. Comparison of the loading functions with an independent data base is performed in Appendix A.

BASIC CONSIDERATIONS

The differential equations describing the steady-state two-dimensional towing configuration and forces in a cable-body system are well defined based on certain simplifying assumptions.² Solutions can be obtained by numerical integration³ requiring as inputs:

1. Tension and angle at some point on the cable, usually an end condition specified at the towed body termination,
2. The form of the hydrodynamic loading functions, and
3. The characteristic drag coefficient for the towline.

The body forces defining the cable end condition typically are measured quite accurately in towing basins or wind tunnels.

¹A complete list of references is given on page 21.

Thus the problem of predicting the steady-state towing configuration becomes one of expressing the hydrodynamic force on the towcable. As noted previously, DTNSRDC has developed a method for directly measuring the hydrodynamic loading functions in (two-dimensional) towing basin experiments. These measured loading functions must ultimately be verified by at-sea measurements since there are some artificialities introduced with the two-dimensional model. In time, as this verification process proceeds on different designs, confidence in the two-dimensional measurements as a basis for loading functions will grow and the need for at-sea verification diminish.

The second method is based on an at-sea experiment in which measurements are made of cable tension, body depth, and cable angle, all as functions of cable scope and speed. The computer model is then exercised assuming different values of hydrodynamic loading until an acceptable match of predicted-to-measured configurations obtains. This regression analysis method is used here to develop ribbon cable loading functions.

A towcable configuration can be defined mathematically by specifying an end condition (tension and angle) and by knowledge of the loading along its span in terms of the normal, Q, and tangential, P, force components expressed as follows:²

$$\begin{aligned} Q &= F - w \sin \phi \\ P &= G - w \cos \phi \end{aligned} \tag{1}$$

where F is the normal component of hydrodynamic force per unit length,
G is the tangential component of hydrodynamic force per unit length,
w is the cable weight in water per unit length, and
 ϕ is the cable angle relative to horizontal.

The effort of this report is to evaluate these expressions of P and Q for the ribbon towcable. Since the weight of cable is readily measured the task becomes one of determining by regression analysis the normal and tangential hydrodynamic force components which produce a fit of computed-to-measured data and which can be expressed as:

$$\begin{aligned} F &= f_n(\phi) \cdot R \\ G &= f_t(\phi) \cdot R \end{aligned} \tag{2}$$

where $f_n(\phi)$ is the normal hydrodynamic loading function,
 $f_t(\phi)$ is the tangential hydrodynamic loading function,
 R is the cable drag per unit length when the axis is 90° to the
 flow ($R = \frac{1}{2}\rho C_R V^2 d$),
 ρ is the density of seawater,
 C_R is the normal drag coefficient based on cable diameter,
 V is velocity, and
 d is cable diameter.

As seen in Equation (2), F and G are expressed as the products of two terms. Essentially the process of determining the hydrodynamic loading functions is one of assuming various forms of $f_n(\phi)$ and $f_t(\phi)$ until, through the regression analysis, a value of C_R (as a function only of Reynolds number) is obtained for which the computed configurations match those measured. Since the fitting process is based on the products $f_n(\phi) \cdot R$ and $f_t(\phi) \cdot R$, it appears that there could be a family of solutions rather than a unique solution. However a constraint on the range of solutions is that the C_R values be plausible. Nonetheless it must be recognized that the derived value of C_R may be different from that which would be obtained by physical measurement and, therefore, it is not valid to imply that this C_R is a characteristic of the cable independent of the hydrodynamic loading functions.

The above caveats notwithstanding, there is confidence in this technique for developing the hydrodynamic loading functions and in applying these functions to the configuration predictions of ribbon towcable provided:

1. the ribbon towcable design is similar,
2. cable diameter is not greatly different from that measured, and
3. the Reynolds number is within the range from 5.2×10^4 to 1.28×10^5 .

In conformance with established methodology,⁴ $f_n(\phi)$ and $f_t(\phi)$ are represented in this analysis by selected terms from the following trigonometric series:

$$f(\phi) = A_0 + A_1 \cos \phi + A_2 \sin \phi + A_3 \cos 2\phi + A_4 \sin 2\phi.$$

DESCRIPTION OF EXPERIMENTAL EQUIPMENT

The experimental equipment consisted of a towed depressor body and the experimental ribbon towcable. The towed body is shown in Figure 1; its dimensions are given in Figure 2. This depressor weighs 1609 pounds (7204 N) in water and has a variable incidence mid-wing. For this experiment, the wing incidence angle was set at -5° (leading edge down). The hydrodynamic performance of the body as measured in the towing basin is shown in Figure 3.

The ribbon towcable consisted of a 1450-ft (442-m) length of 0.78-inch (1.98 cm) diameter, double-armored, electrical-mechanical cable with ribbons attached, as shown in Figure 4. The cable consisted of two layers, reverse lay, of galvanized steel armor strands surrounding a 10-conductor electrical core. The cable weighed 0.688 pounds per foot (1.02 kg/m) in sea water and had a breaking strength of approximately 50,000 pounds (223,880 N). The ribbons were polyurethane strips threaded under the outer layers of armor. Ribbon geometry is given in Table 1.

TABLE 1 - CABLE AND RIBBON GEOMETRY

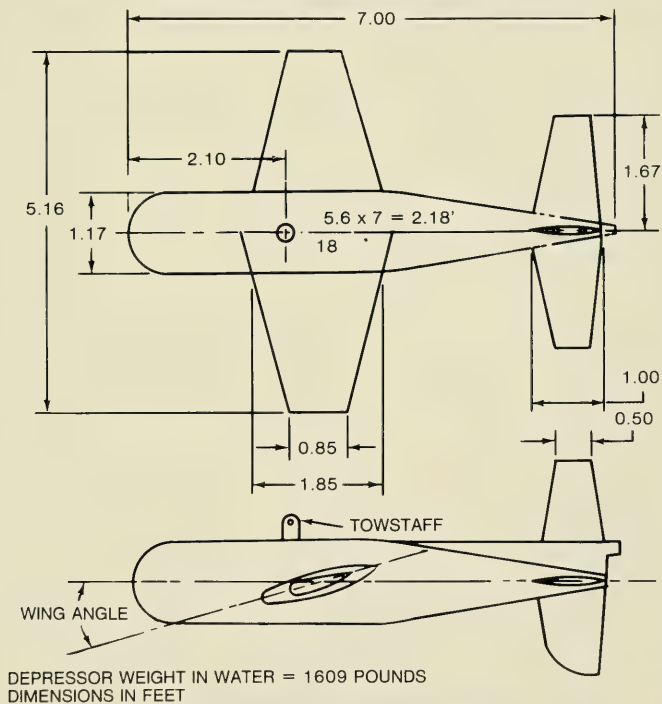
Cable diameter	0.78 in. (1.98 cm)
Cable length	1450 ft. (442 m)
Ribbon loop length	9.36 in. (23.77 cm)
Ribbon length-to-cable-diameter ratio	6
Ribbon width	0.78 in. (1.98 cm)
Material thickness	0.015 in. (.038 cm)
Spacing (centers)	0.78 in. (1.98 cm)
Ribbon coverage	100%

The towcable was marked at 100-ft (30.5-m) intervals to permit estimation of cable scope in the water to about ± 5 ft (± 1.5 m).



PSD 0053/25-10-77

Figure 1 - DTNSRDC Depressor



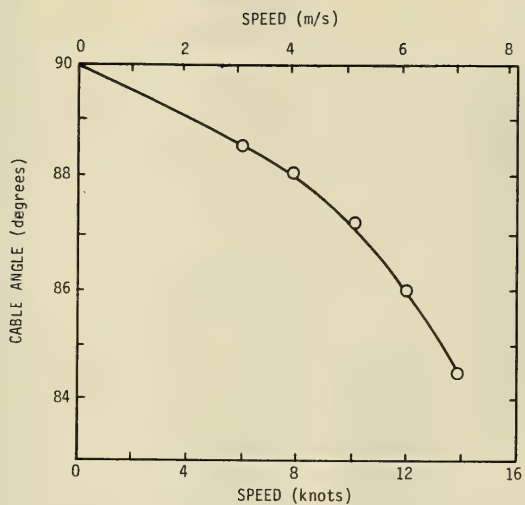


Figure 3a - Cable Angle at the Depressor

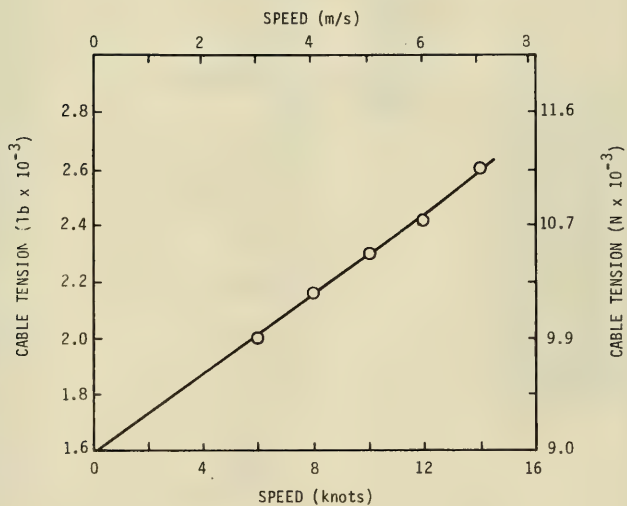
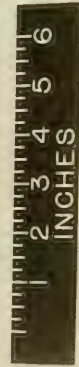


Figure 3b - Cable Tension at the Depressor

Figure 3 - Depressor Performance as a Function of Speed for a Wing Angle of -50



PSD 340261

Figure 4 - Typical Ribbon Towcables

DESCRIPTION OF INSTRUMENTATION

The experimental system was instrumented to measure the following parameters:

1. body depth below the water surface,
2. cable tension at the ship, and
3. towing speed.

A watertight instrument housing in the depressor body contained electronics for amplification and remote electrical calibration of the body depth sensor. The housing also contained a voltage-controlled oscillator-type telemetry assembly to transmit the depth signal through the towcable to the graphic and digital recorders aboard ship. The cable tension at the ship sensor was direct wired to a control unit within the ship laboratory which contained the tension sensor amplifier and electrical calibration circuit. Ship speed was measured by the DTNSRDC knotmeter. The sensors and their accuracies are listed in Table 2.

TABLE 2 - MEASUREMENT SENSORS

Measured Parameter	Sensor		Measurement Accuracy
	Type	Range	
Cable tension at the ship	Dyna-Line tensiometer	0-10,000 lb	\pm 200 lb
Body depth	Diaphragm pressure gage	0-1125 ft	\pm 5.6 ft
Ship speed	DTNSRDC knotmeter	0-25 kts	\pm 0.01 kt

The design of the electrical calibration circuits in this measurement system virtually eliminate the effect of long-term zero drift and sensitivity error within the amplifier and recording electronics external to the sensors. As a result the total readout error is limited to that of each individual sensor. These calibration principles are discussed in detail in Reference 5. The ship-board readout electronics consisted of a 6-channel strip chart recorder providing a time history of cable tension at the ship, depth of the body, and ship speed; an integrating digital voltmeter, and two preset electronic counters provided digital displays of the cable tension, body depth, and ship speed, respectively. A digital recorder was used in conjunction with the digital display units to obtain a printed record of the data.

EXPERIMENTAL ARRANGEMENT AND PROCEDURES

The experiment was conducted at sea from the R/V PATRICK KILEY in the New Providence Channel off the Bahamas during July 1970. The operational area was selected for minimum sea state conditions to obtain, as nearly as practicable, steady-state towing.

The general towing arrangement is shown in Figure 5. A cable dominated system was chosen assuring curvature over a significant portion of the towline. Use of the AN/SQA-13(XN-1) winch and handling system accommodated the large size towcable and simplified system deployment and retrieval.

The system was towed in a calm sea at nominal speeds of 6, 8, 10, 12 and 14 knots (3.1, 4.1, 5.1, 6.2, and 7.2 m/s). At each speed, measurements were taken at nominal wetted cable scopes of 200, 400, 600, 800 and 1000 ft (61, 122, 183, 244 and 305 m).

Prior to recording data for each new speed and scope, body depth was monitored to assure that the system had established a new equilibrium configuration and was no longer influenced by speed change transients. Four separate sets of measurements were taken for each data run.

RESULTS AND DISCUSSION

The averaged measured values of cable tension at the ship and depressor are shown in Figures 6 and 7. Also shown in the figures are computer model predictions (solid lines) based on a regression-analysis determination of the hydrodynamic loading functions f_n and f_t and the drag coefficient C_R . These functions represent the best fit to the data and were obtained through a trial and error process. The values of the functions are:

$$f_n = 0.4986 - 0.2499 \cos\phi + 0.2527 \sin\phi - 0.2487 \cos 2\phi \quad (4)$$

$$f_t = -0.2255 + 0.3417 \cos\phi + 0.2255 \sin\phi - 0.0811 \sin 2\phi \quad (5)$$

$$C_R = 5.7467 - 0.93 \log_{10} R_e \quad (6)$$

These functions are shown graphically in Figures 8 and 9 and apply to the Reynolds number range from 5.2×10^4 to 1.28×10^5 . In assessing the goodness of fit of computed-to-measured data it is seen that tension predictions are generally within 10% of measured values with the body force zeroed out (within 5% with body force included). Body depth predictions are within 5% of measured values except

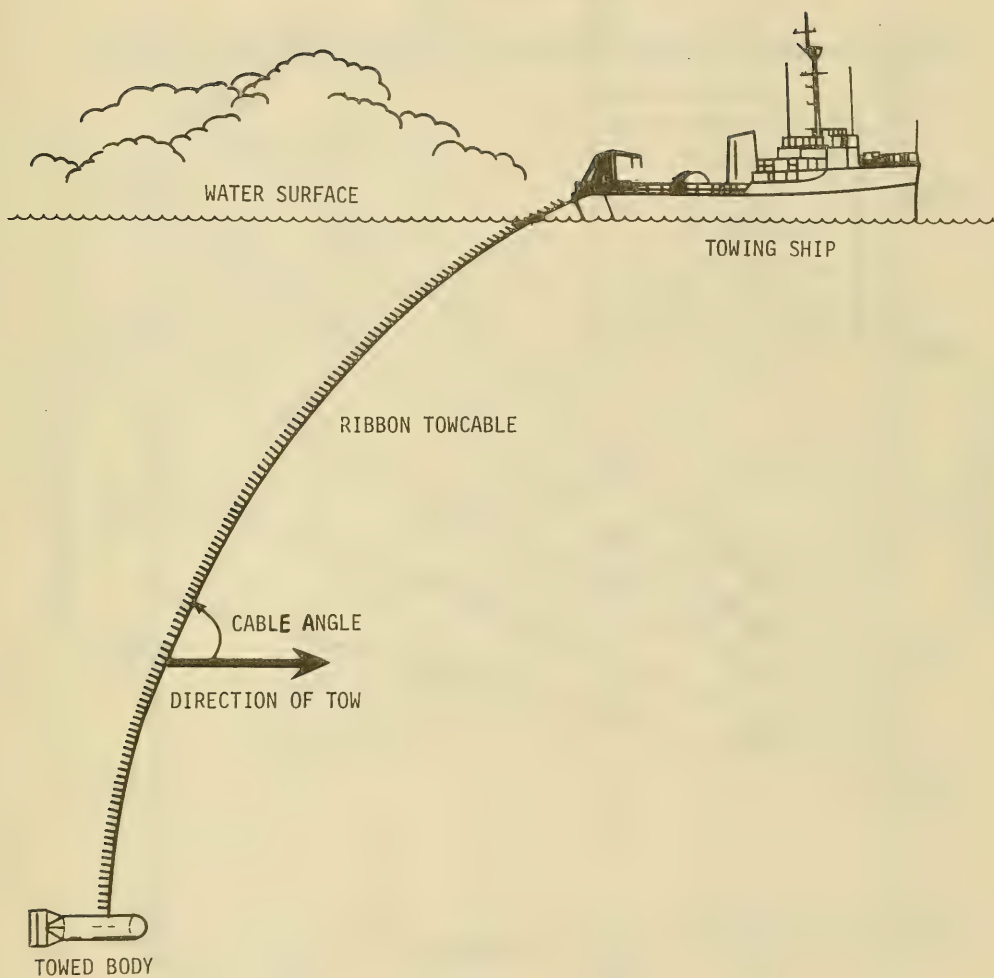


Figure 5 - Schematic Diagram of the Towing Arrangement

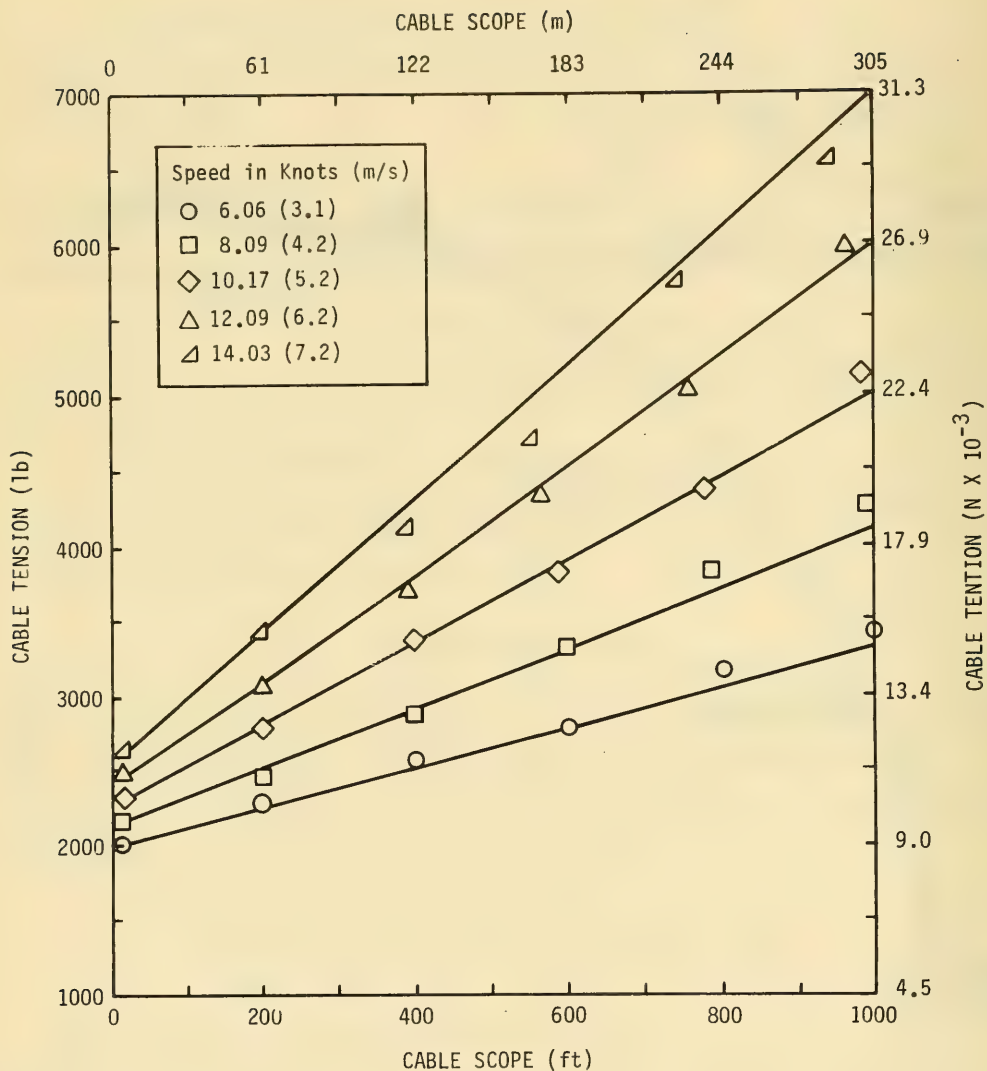


Figure 6 - Cable Tension at the Ship as a Function of Cable Scope

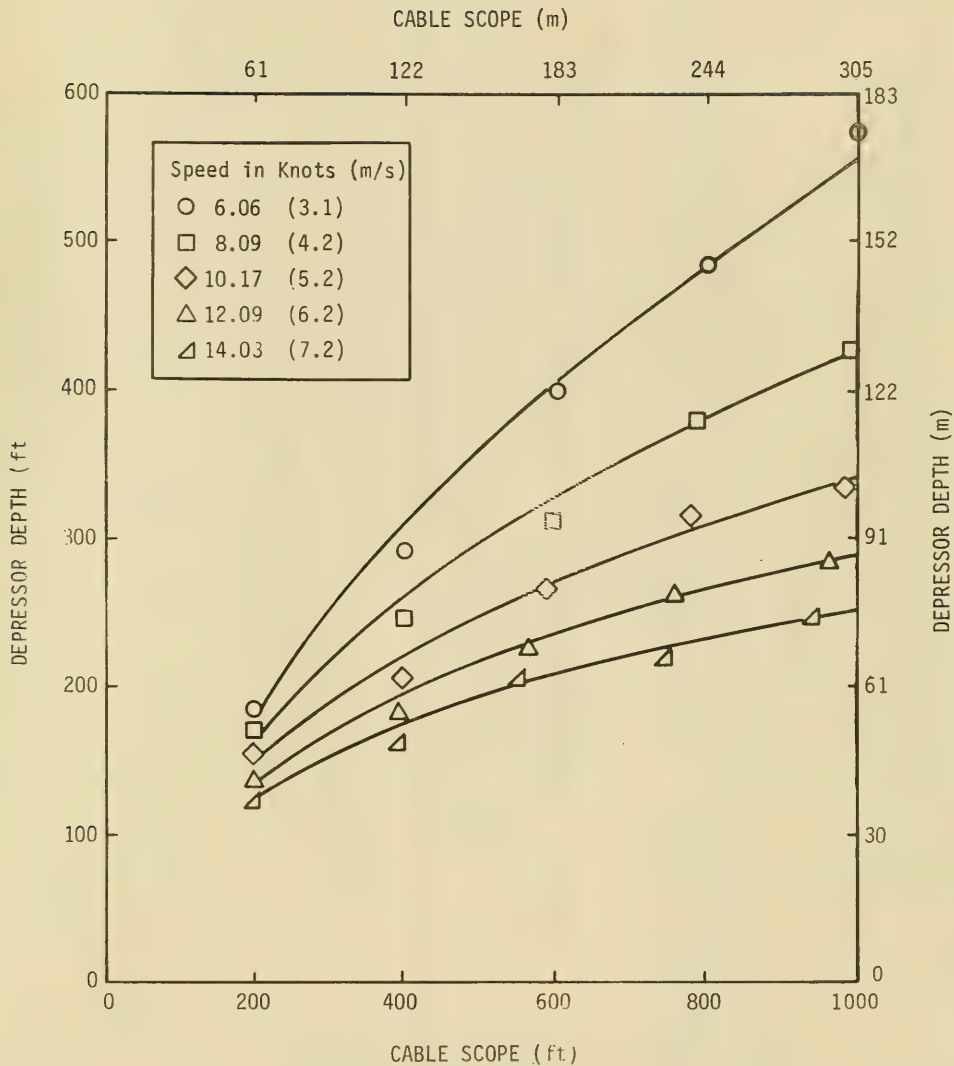


Figure 7 - Depressor Depth as a Function of Cable Scope

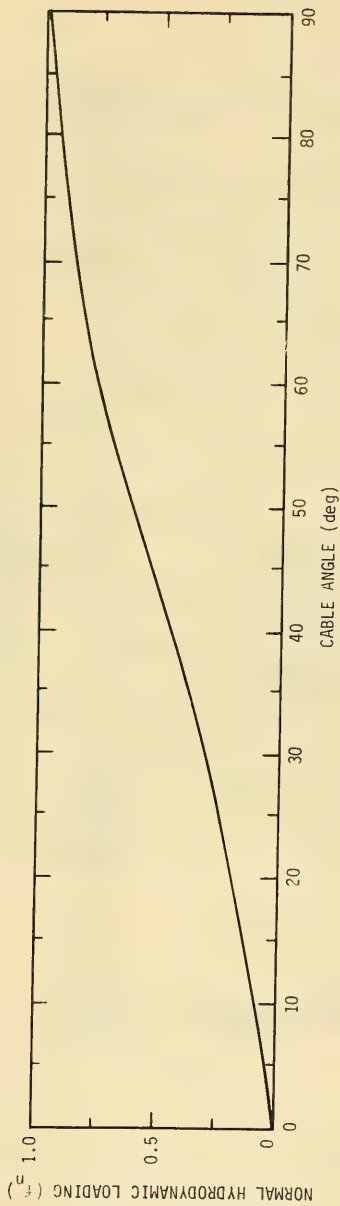


Figure 8a - Normal Hydrodynamic Loading Function vs Cable Angle

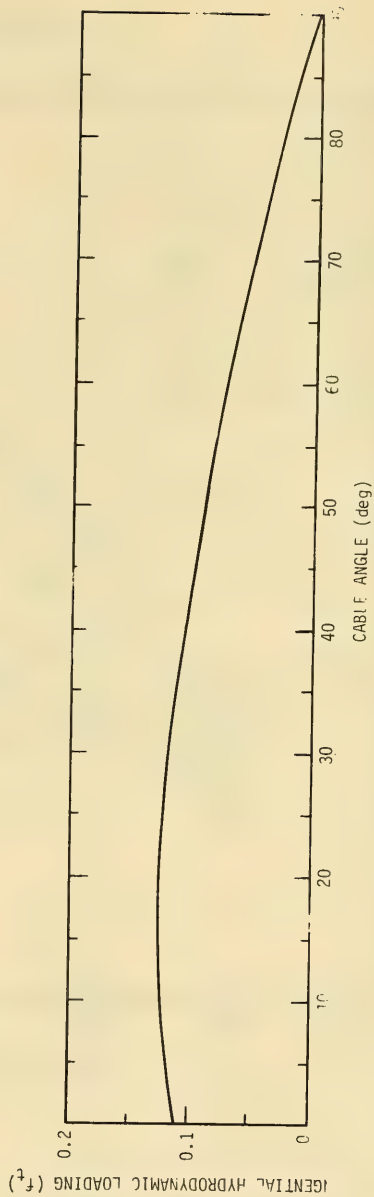


Figure 8b - Tangential Hydrodynamic Loading Function vs Cable Angle

Figure 8 - Hydrodynamic Loading Functions

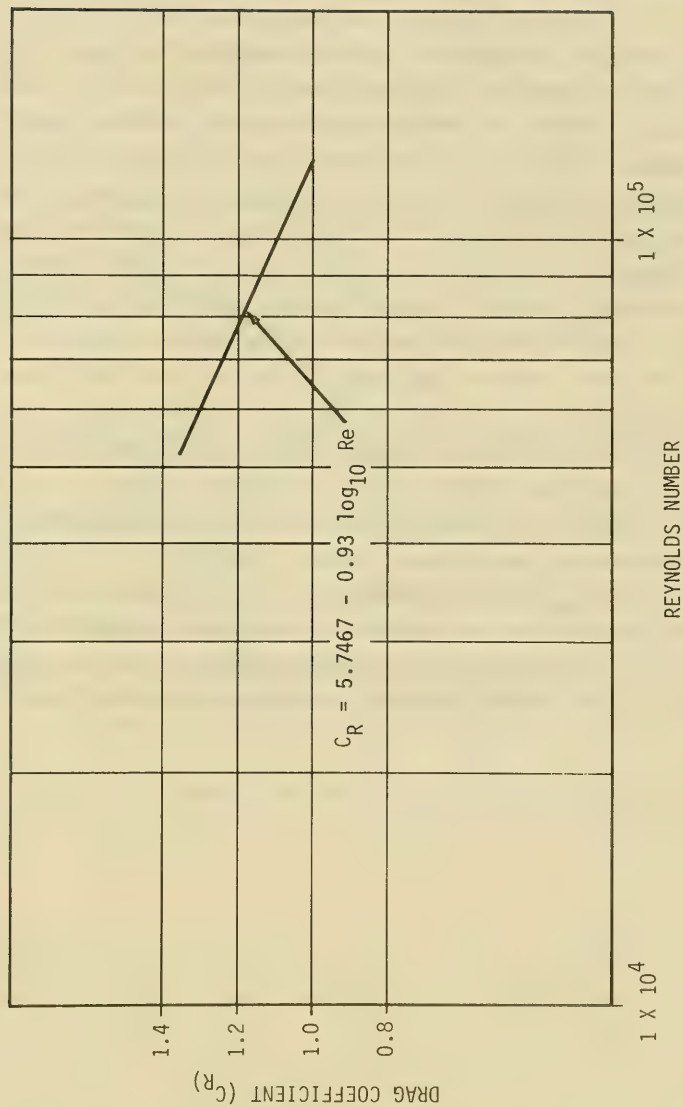


Figure 9 - Drag Coefficient as a Function of Reynolds Number

for scopes of 400 and 200 feet where the average differences are about 6% and 8.7% respectively.

The relationships between $f_n(\phi)$, $f_t(\phi)$ and C_R have been discussed previously. With respect to the problem of fitting predicted-to-measured configurations another factor should be considered. In this methodology the term C_R accounts for the effect of Reynolds number on both the normal and tangential components of hydrodynamic force. However, it should not be expected that the Reynolds number effects are physically the same for the normal component at steep cable angles where pressure drag predominates and for the tangential component at shallow angles where frictional drag predominates. The final curve fits shown in Figures 6 and 7, therefore, reflect a compromise in the expression of C_R with Reynolds number.

Ribbon represents a type of "fairing" unlike streamlined rigid fairing in that the geometry changes with speed and with cable angle inclination. It has been observed that at an angle of the cable 90° to the flow, the ribbons stream out normal to the cable axis. At shallow angles, the ribbons have been observed to lay down along the trailing edge of the cable. In addition to cable angle, intuitively such factors as ribbon material stiffness, percent cable coverage, and method of attachment are judged to influence the detailed geometry of the ribbons and therefore the hydrodynamic loading. Some insight into this is given in Appendix A. However, primarily because of a lack of knowledge of how to scale the material stiffness factor, caution must be exercised in applying these loading functions to a cable of significantly different diameter. Scaling should not be attempted outside of the Reynolds number range covered in these tests.

CONCLUSIONS

As a result of this experiment and the data analysis here and in the Appendix the following is concluded;

1. The derived hydrodynamic loading functions and drag coefficients will support a good estimate of towing configurations for this design of ribbon towcable and for the range of variables covered by the experiment.
2. The functions and coefficients should be applied to other cable diameters and/or ribbon designs with caution since ribbon material thickness appears to be an influential parameter and methods for scaling material stiffness have not been developed.

REFERENCES

1. Folb, R., "Experimental Determination of Hydrodynamic Loading for Ten Cable Fairing Models," DTNSRDC Report 4610, November 1975.
2. Pode, L., "Tables for Computing the Equilibrium Configuration of a Flexible Cable in a Uniform Stream," David Taylor Model Basin Report 687, March 1951.
3. Cuthill, E.H., "A FORTRAN IV Program for the Calculation of the Equilibrium Configuration of a Flexible Cable in a Uniform Stream," Naval Ship Research and Development Center Report 2531, February 1968.
4. Springston, G., "Generalized Hydrodynamic Loading Functions for Bare and Faired Cable in Two-Dimensional Steady-State Cable Configurations," Naval Ship Research and Development Center Report 2424, June 1967.
5. Singleton, R.J., "BIAS Buoy Measurement and Depth Control Instrumentation," David Taylor Naval Ship Research and Development Center Report 4451, November 1975.

APPENDIX A

A COMPARISON OF THE HYDRODYNAMIC LOADING FUNCTIONS WITH SOME CRITICAL ANGLE TOWING DATA

Figures A1 and A2 show hydrodynamic data on ribbon towcables obtained in critical angle towing tests by DTNSRDC. In these experiments long lengths of cable were towed at the critical angle while cable tension at the towpoint, cable angle and speed were measured. From these data a few points can be extracted for comparison with the hydrodynamic loading functions and drag coefficients developed earlier in the body of this report.

Two ribbon towcable models were evaluated, the models differing primarily in the thickness of the ribbon material. Models A and B each had a 0.84-in. (21.3-mm) diameter, double-armored electrical cable weighing 1.02 lb/ft (1.51 kg/m) in sea water. Ribbon configurations were as shown in Table A.1.

TABLE A.1 - RIBBON CONFIGURATIONS

MODEL	RIBBON LENGTH	RIBBON WIDTH	MATERIAL THICKNESS	% CABLE COVERAGE
A	6D	2D	15 mil (0.38 mm)	50
B	6D	2D	30 mil (0.76 mm)	50

The ribbon material was polyurethane and the ribbon density (or percent cable coverage) was 50% compared to 100% for the model described in the body of the present report. Note, however, that the latter model and Model A have the same material thickness, namely 15 mil (0.38 mm) which is one-half the material thickness for Model B.

In reviewing Figures A1 and A2, which are the reduced hydrodynamic measurements of towcable tension per unit length and towing angle, it can be seen that the Model B cable tows at a more shallow angle and develops a much higher tension than the Model A cable. (In the graphs showing 30-mil (0.76-mm) thick ribbon cable data Model B refers to the curve marked R/S = 50/00. The other curves result from parts of the test in which increasing percentages of the ribbon were clipped off.)

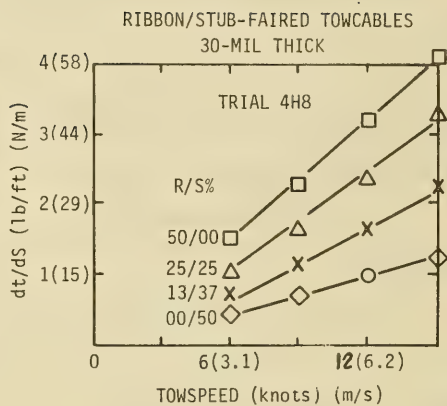
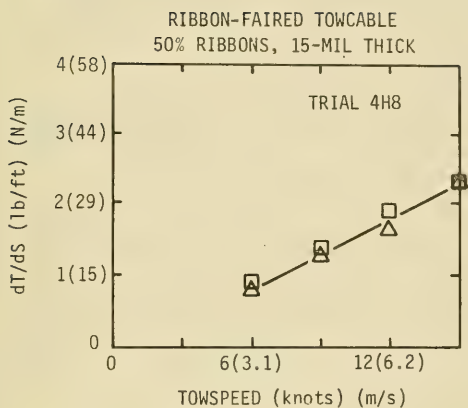


Figure A.1 - Towable Tension per Unit Length
versus Towspeed for Various Towcables

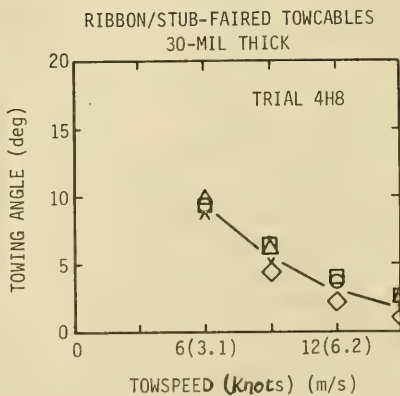
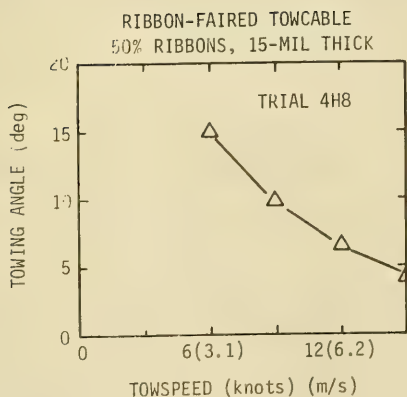


Figure A.2 - Towing Angles versus Towspeed for Various Towcables

Since these cables are trailing at a constant angle for each speed, each experimental data point yields a set of hydrodynamic loading data points which can be compared with the functions (or coefficients) developed earlier. Considering the normal components of force first, in a critical angle to the normal component of hydrodynamic force balances the cable weight component normal to the cable axis. Thus

$$(f_n)_{\phi_c} \cdot R = w \cdot \cos \phi_c \quad (1A)$$

from which

$$C_R = \frac{w \cdot \cos \phi_c}{(f_n)_{\phi_c} (\frac{1}{2} \rho V^2 d)} \quad (2A)$$

where ϕ_c is the critical angle.

Applying the normal hydrodynamic loading function presented in equation (4), C_R 's were computed for the two models from the data shown in Figure A.2 and are presented in Table A.2.

TABLE A.2 - DERIVED NORMAL DRAG COEFFICIENTS

Speed (kt)	Reynolds Number	Model A		Model B		C_R^*
		ϕ_c	C_R	ϕ_c	C_R	
6	5.9×10^4	15°	1.28	9°	2.56	1.31
9	8.86×10^4	10°	0.99	5.8°	1.97	1.15
12	1.17×10^5	6.5°	0.96	4°	1.71	1.03
15	1.477×10^5	4.5°	0.96	2.5°	1.86	0.94

Also shown in Table A.2 is a column designated C_R^* . These values of C_R were computed by equation (6) for the corresponding Reynolds number in Table A.2. It is seen that C_R^* and C_R for Model A agree rather well. It is concluded that the representation of the normal hydrodynamic force developed in the body of the report is also a good representation for Model A. This is in spite of the fact that Model A has only 50% of the ribbon cable coverage. The reason may be that the data base is comprised largely of shallow angle data. It has been observed that at

shallow angles ribbons tend to lie flat along the trailing edge of the cable. This may reduce the effect of percent cable coverage on the normal component of hydrodynamic force.

In the case of Model B the derived drag coefficients C_R are approximately double the values for Model A (and C_R^*) a trend which could be inferred from the data in Figure A.2.

It may be that the thicker (stiffer) ribbon material results in a higher projected frontal area to the flow and this accounts for the higher drag coefficients when based on cable diameter. Or it may be that material stiffness alters the wake to the extent that a different loading function applies or some combination of the two. Regardless, it is clear that the normal hydrodynamic loading function and C_R derived from a 15 mil (0.38 mm) ribbon data base is a poor representation for a towcable with 30 mil (0.76 mm) ribbon.

In analyzing the tangential hydrodynamic force components, estimates of tangential hydrodynamic loading function values can be made from the data in Figure A.1 and the following relation:

$$(f_t)_{\phi_c} = \frac{(\Delta T / \Delta S - w \sin \phi_c)}{R} \quad (3A)$$

Computed values of $(f_t)_{\phi_c}$ are shown in Table A.3.

TABLE A.3 - TANGENTIAL HYDRODYNAMIC LOADING VALUES

Speed (kt)	Model A				Model B			
	ϕ_c	$\Delta T / \Delta S$	R	f_t	ϕ_c	$\Delta T / \Delta S$	R	f_t
6	15°	0.9	9.19	0.069	9°	1.6	18.39	0.078
9	10°	1.3	16.00	0.070	5.8°	2.2	31.83	0.066
12	6.5°	1.9	27.58	0.065	4°	3.2	49.12	0.64
15	4.5°	2.3	43.09	0.052	2.5°	4.1	83.49	0.049

The computed values of $f_t(\phi)$ are also plotted in Figure A.3. Considering the values of $f_t(\phi)$ as derived from the three data bases, neglecting for the moment the C_R values by which they were derived and how the C_R values ultimately scale the tangential hydrodynamic force, there is a consistency to the $f_t(\phi)$ values. First, Models A and B both representing 50% ribbon coverage have $f_t(\phi)$ values which closely approximate a single trend line (Figure A.3). Second, these values are approximately one-half those pertaining to the 100% ribbon coverage cable. So it appears that wetted surface (percent cable coverage) is a key parameter controlling tangential drag as would be expected.

However to compute the tangential force C_R must be applied. If only the 15 mil (0.38 mm) thick ribbon models are considered, the consistency is maintained and so is the concept of surface area as a key parameter. When the 30 mil (0.76 mm) case is considered with its large C_R values the tangential force scales up to where the 30 mil (0.76 mm) ribbon tangential force is twice that of the 15 mil (0.38 mm) ribbon although both have the same wetted surface. Now the concept of wetted surface area having a linear effect on tangential force does not hold.

It must be concluded that the characteristics of the ribbon especially material stiffness and possibly method of attachment are influencing hydrodynamic forces both normal and tangential in important ways that are not understood. For this reason scaling this data to ribbon cables of significantly different size must be done with caution.

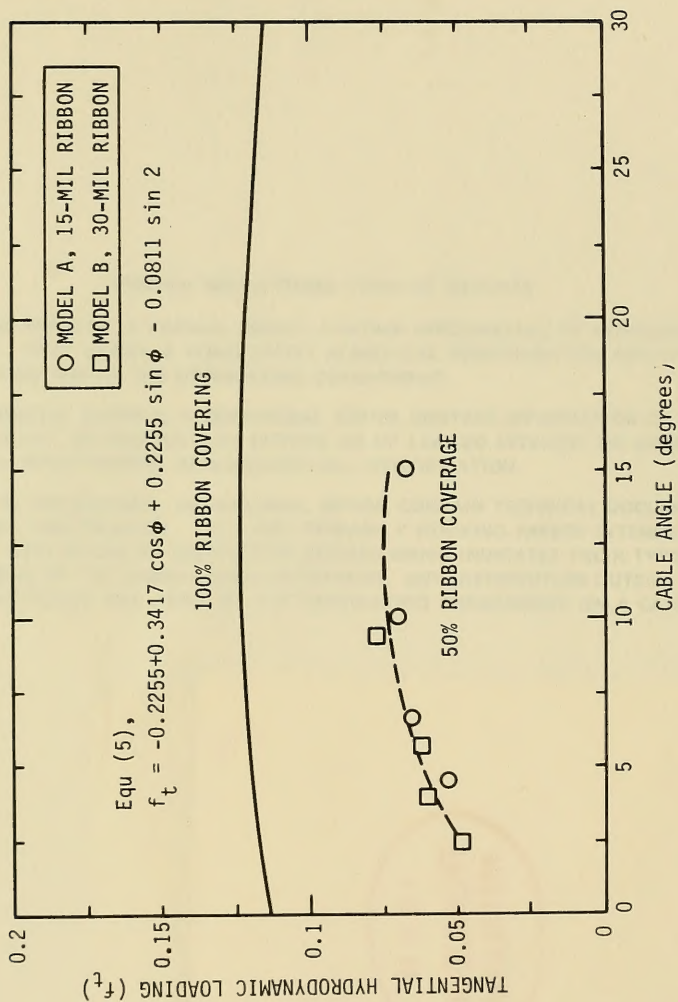


Figure A.3 - Tangential Hydrodynamic Loading vs Cable Angle

DTNSRDC ISSUES THREE TYPES OF REPORTS

1. DTNSRDC REPORTS, A FORMAL SERIES, CONTAIN INFORMATION OF PERMANENT TECHNICAL VALUE. THEY CARRY A CONSECUTIVE NUMERICAL IDENTIFICATION REGARDLESS OF THEIR CLASSIFICATION OR THE ORIGINATING DEPARTMENT.

2. DEPARTMENTAL REPORTS, A SEMIFORMAL SERIES, CONTAIN INFORMATION OF A PRELIMINARY, TEMPORARY, OR PROPRIETARY NATURE OR OF LIMITED INTEREST OR SIGNIFICANCE. THEY CARRY A DEPARTMENTAL ALPHANUMERICAL IDENTIFICATION.

3. TECHNICAL MEMORANDA, AN INFORMAL SERIES, CONTAIN TECHNICAL DOCUMENTATION OF LIMITED USE AND INTEREST. THEY ARE PRIMARILY WORKING PAPERS INTENDED FOR INTERNAL USE. THEY CARRY AN IDENTIFYING NUMBER WHICH INDICATES THEIR TYPE AND THE NUMERICAL CODE OF THE ORIGINATING DEPARTMENT. ANY DISTRIBUTION OUTSIDE DTNSRDC MUST BE APPROVED BY THE HEAD OF THE ORIGINATING DEPARTMENT ON A CASE-BY-CASE BASIS.

